New Phytologist

Polyploidization leads to salt stress resilience via ethylene signaling in citrus plants

Xin Song[1,2]*, Miao Zhang[1,3]*, Ting-Ting Wang[1], Yao-Yuan Duan[1], Jie Ren[1], Hu Gao[1], Yan-Jie Fan[1], Qiang-Ming Xia[1,2], Hui-Xiang Cao[1], Kai-Dong Xie[1], Xiao-Meng Wu[1], Fei Zhang[1,4], Si-Qi Zhang[3], Ying Huang[5], Adnane Boualem[3,6], Abdelhafid Bendahmane[3,6], Feng-Quan Tan[1,3] and Wen-Wu Guo[1,4]

[1]National Key Laboratory for Germplasm Innovation & Utilization of Horticultural Crops, College of Horticulture & Forestry Sciences, Huazhong Agricultural University, Wuhan, 430070, China; [2]Hubei Key Laboratory of Germplasm Innovation and Utilization of Fruit Trees, Institute of Fruit and Tea, Hubei Academy of Agricultural Science, Wuhan, 430064, China; [3]Institute of Plant Sciences Paris-Saclay (IPS2), Université Paris-Saclay, CNRS, INRAE, Université Evry, Gif sur Yvette, 91190, France; [4]Hubei Hongshan Laboratory, Wuhan, 430070, China; [5]Institute of Science and Technology (IST), Klosterneuburg, 3400, Austria; [6]The Sino-French International Joint Laboratory for Horticultural Research, Huazhong Agricultural University, INRAE, ENS de Lyon, Université Paris-Saclay, Wuhan, 430070, China

Authors for correspondence:
Feng-Quan Tan
Email: fengquan.tan@universite-paris-saclay.fr

Wen-Wu Guo
Email: guoww@mail.hzau.edu.cn

Received: *24 October 2024*
Accepted: *12 January 2025*

New Phytologist (2025) **246:** 176–191
doi: 10.1111/nph.20428

Key words: ethylene, perennial woody plant, polyploid, root architecture, salt tolerance.

Summary

- Polyploidization is a common occurrence in the evolutionary history of flowering plants, significantly contributing to their adaptability and diversity. However, the molecular mechanisms behind these adaptive advantages are not well understood.
- Through comprehensive phenotyping of diploid and tetraploid clones from *Citrus* and *Poncirus* genera, we discovered that genome doubling significantly enhances salt stress resilience. Epigenetic and transcriptomic analyses revealed that increased ethylene production in the roots of tetraploid plants was associated with hypomethylation and enhanced chromatin accessibility of the *ACO1* gene. This increased ethylene production activates the transcription of reactive oxygen species scavenging genes and stress-related hormone biosynthesis genes. Consequently, tetraploid plants exhibited superior root functionality under salt stress, maintaining improved cytosolic K^+/Na^+ homeostasis.
- To genetically validate the link between salt stress resilience and *ACO1* expression, we generated overexpression and knockout lines, confirming the central role of *ACO1* expression regulation following genome doubling in salt stress resilience.
- Our work elucidates the molecular mechanisms underlying the role of genome doubling in stress resilience. We also highlight the importance of chromatin dynamics in fine-tuning ethylene gene expression and activating salt stress resilience pathways, offering valuable insights into plant adaptation and crop genome evolution.

Introduction

Polyploidization, the process of genome doubling, has been pivotal in the evolution of flowering plants, greatly contributing to their adaptability, diversity, and survival (Otto & Whitton, 2000; Van de Peer *et al.*, 2017; Köhler *et al.*, 2021). Polyploid plants frequently display enhanced genetic variation, increased cell size, and new traits that offer a selective advantage under various environmental stresses (Soltis & Soltis, 2000; Chen, 2007; Allario *et al.*, 2013; Del Pozo & Ramirez-Parra, 2014; Van de Peer *et al.*, 2020; Wang *et al.*, 2021). However, the mechanisms by which genome doubling, without altering genes, can reprogram gene expression to prime resilience remain unclear.

Salinity presents a severe abiotic stress in soil environments, impacting over 7.5% of the global land (Liang *et al.*, 2024) and significantly curtailing the growth, productivity, and survival of major cereal (Yu *et al.*, 2023) and horticultural crops (Moya *et al.*, 2003; Delarue *et al.*, 2025). Salt stress, especially from high sodium chloride (NaCl) levels, disturbs the homeostasis of sodium (Na^+) and potassium (K^+) ions within plant cells, which is essential for maintaining cellular functions (Almeida *et al.*, 2017). When this balance is disturbed, it triggers a cascade of harmful effects, one of the most detrimental being the excessive accumulation of reactive oxygen species (ROS) (Allakhverdiev *et al.*, 2002; Shabala & Cuin, 2008).

Roots are the first to detect and respond to salt stress (Galvan-Ampudia Carlos *et al.*, 2013). Their ability to adjust architecture and maintain functionality in response to salt stress has been harnessed to improve crop resilience (Zhan *et al.*, 2015; Ma *et al.*, 2018; Lynch, 2022; Hostetler *et al.*, 2023). Although the diversity in root system types suggests an evolutionary trend toward enhanced flexibility and adaptability under

*These authors contributed equally to this work.

environmental pressures, such as soil salinity (Galvan-Ampudia & Testerink, 2011; Van Zelm *et al.*, 2020), how polyploidization affects root resilience is unclear.

Ethylene, a gaseous plant hormone, has a central role in root development, yet its role in resilience to salt stress is not well understood (Achard *et al.*, 2006; Schmidt *et al.*, 2013; Dubois *et al.*, 2018). Ethylene biosynthesis proceeds from S-adenosylmethionine through two dedicated enzymes: 1-aminocyclopropane-1-carboxylic (ACC) synthase (ACS) and ACC oxidase (ACO) (Yang & Hoffman, 1984). While ACS is considered the rate-limiting step in ethylene biosynthesis, several studies suggest that ACO also serves as a control point under specific developmental and stress conditions in various plant species (Qin *et al.*, 2007; Linkies *et al.*, 2009). Additionally, genes involved in ethylene biosynthesis and signaling appear to be preferentially retained after natural polyploidization, highlighting their critical role in plant adaptation (Jourda *et al.*, 2014; Tasdighian *et al.*, 2017).

Annual plants have evolved various strategies to tolerate or avoid soil environmental stresses through rapid growth and reproduction (Franks *et al.*, 2007; Franks, 2011). By contrast, perennial plants must adapt their root systems to cope with various soil challenges, leading to different evolutionary trends in root systems between perennial and annual plants (Schenk & Jackson, 2002; Kong *et al.*, 2014). Annual plants typically have a fibrous root system with thin, thread-like roots forming a dense network near the soil surface, whereas perennial trees often exhibit a taproot system with thicker roots penetrating deep into the soil (Roumet *et al.*, 2006; Hummel *et al.*, 2007). While the impacts of polyploidization on root systems and plant adaptability remain unclear, it is evident that genome doubling influences root system development differently in perennial woody plants compared with herbaceous annuals.

In this study, we used three woody perennial crops of *Citrus* and *Poncirus* genera, as model systems to investigate how polyploidization contributes to salt stress resilience in woody plants. Utilizing the apomictic reproduction system of these species, which can result in spontaneous tetraploidization, we generated plants that are genetically identical clones but differ in ploidy levels (Allario *et al.*, 2011; Tan *et al.*, 2017). We assessed their root architecture, salt stress resilience, and the underlying molecular mechanisms. Our research highlights the role of chromatin remodeling following polyploidization in driving developmental and physiological changes associated with salt stress resilience.

Materials and Methods

Plant materials and growth conditions

We used diploid and tetraploid *Citrus* rootstocks in *Citrus reticulata* Blanco, *C. junos* Sieb. ex Tanaka, and *Poncirus trifoliata* L. Raf. backgrounds. Tetraploids were identified among a population of seedlings derived from the corresponding diploid genotypes at the National Citrus Breeding Center at Huazhong Agricultural University (Tan *et al.*, 2015, 2017). Diploid *C. junos* were used for genetic transformations. All plants were cultured in 0.5 × Hoagland nutrient solution or commercial soil in a growth chamber at 25°C under a 16 h : 8 h, light : dark photoperiod.

Phylogenetic analysis

The species phylogenetic tree was constructed using genome-wide SNP data from 11 citrus accessions (Supporting Information Table S1). Clean reads were mapped to the *Citrus sinensis* v.3.0 or *P. trifoliata* v.1.0 genome (http://citrus.hzau.edu.cn/) using BWA (Li & Durbin, 2010). High-quality SNPs were identified using the Genome Analysis Toolkit (GATK) v.4.1.2 (McKenna *et al.*, 2010) and subsequently used to construct a phylogenetic tree with IQ-TREE v.2.0 (Nguyen *et al.*, 2015) under the GTR + I + G model, with 1000 bootstrap replicates and default settings. The maximum likelihood tree was rooted with *Clausena lansium* as the outgroup and visually validated using the Interactive Tree of Life Tool. For the phylogenetic tree of ACOs protein, sequences from different species were obtained from the PHYTOZOME 13 database (https://phytozome-next.jgi.doe.gov) and were used to perform a search of the *C. sinensis* v.3.0 genome using BLASTP with an *E*-value threshold of 1e-5. The phylogenetic tree was constructed using MEGA7, with default settings and the neighbor-joining method.

Tissue K^+ and Na^+ quantification

Seedlings were cultured on a 0.5× Hoagland nutrient solution either with or without the addition of 200 mM NaCl for 15 d. Roots were washed three times with deionized water before harvest. Roots and shoots were separated and dried at 65°C for 3 d. Dry samples were digested with a mixed solution of acids $HNO_3/HClO_4$ (85/15, v/v). The contents of K^+ and Na^+ were measured by inductively coupled plasma mass spectrometry (PerkinElmer NexION-300×, Waltham, MA, USA).

Root parameter determination

Root systems were washed and blotted dry with soft paper. Subsequently, each root system was segmented and scanned using an Epson Perfection V850 Pro scanner (Epson America Inc.). The scanned images were analyzed using WINRHIZO PRO software to quantify root number, total root length, and mean root diameter.

DAB staining assay and measurement of ROS accumulation and Chl content

DAB staining was performed as described previously (Huang *et al.*, 2013). H_2O_2 content was measured using a H_2O_2 content assay kit (Boxbio, Beijing, China) according to the manufacturer's instructions. Chlorophyll content was measured as described previously (Zhou *et al.*, 2012). Three biological replicates were analyzed with each composed of tissue from three independent plants. One representative data set is shown for each experiment.

Fluorescence detection of ROS in citrus protoplast

Intracellular total ROS were detected using the Reactive Oxygen Species Assay Kit (50101ES01; Yisheng Biotechnology Co., Ltd, Shanghai, China) according to the manufacturer's protocol. Citrus callus protoplasts were transfected with *35S:CjACO1-RFP* and *35S: RFP* (control). The protoplasts were incubated with the WI solution (0.4 M mannitol, 20 mM KCl, 4 mM MES, pH 5.7) in the dark (28°C) for 16 h. The protoplasts were supplemented with 10 μM DCFH-DA (2′,7′-dichlorodihydrofluorescein diacetate) staining for 20 min at 28°C in the darkness and supplemented with 100 μM Rosup for 10 min at 28°C in darkness. Then, the protoplasts were washed several times with the W5 solution (154 mM NaCl, 125 mM $CaCl_2$, 5 mM KCl, and 2 mM MES, pH 5.7) to clear excess dye before imaging. The florescence images were acquired using a Leica TCS SP8 (Leica Microsystems, Wetzlar, Germany) confocal laser scanning microscope with the following wavelength settings: DCF: Excitation = 488 nm, Emission = 505–550 nm; RFP: Excitation = 552 nm, Emission = 580–630 nm.

Sampling for next-generation sequencing analysis

Four-month-old plants were grown on a 0.5× Hoagland nutrient solution supplemented with either 0 mM or 200 mM NaCl. After 15 d, whole roots were harvested for RNA-seq, whole-genome bisulfite sequencing, and ATAC-seq. For RNA-seq analysis of *ACO1* overexpression lines, whole roots were collected from 1-month-old plants. RNA-seq and whole-genome bisulfite sequencing were conducted using three biological replicates, while ATAC-seq utilized two biological replicates. Each replicate consisted of pooled whole roots from two to three plants.

RNA-Seq and qRT-PCR analysis

Total RNA isolation, library construction, and sequencing were performed by Novogene Bioinformatics Technology Co. Ltd. Sequencing was performed on an Illumina HiSeq 4000 platform. Over 73% of the high-quality reads were mapped to the reference genome of *C. sinensis* v.1.1 (Phytozome) using Hisat2 v.2.2.1 with default parameters (Kim et al., 2019) and normalized gene expression levels (fragments per kilobase of transcript per million mapped reads, FPKM) were calculated by Cufflinks v.2.2.1 (Trapnell et al., 2012). Genes with a P-value < 0.05 following Benjamini and Hochberg correction and an absolute value of log2 fold change > 0.58 were considered differentially expressed. Gene Ontology (GO) enrichment analysis was carried out using AgriGO (http://systemsbiology.cau.edu.cn/agriGOv2/). Subsequently, RNA was converted to cDNA using HiScript II Q RT SuperMix for qPCR kit (R223-01; Vazyme, Nanjing, China). Quantitative reverse transcription polymerase chain reaction was performed using a 2× Universal SYBR Green Fast qPCR Mix (RM21203; ABclonal, Wuhan, China). All data were normalized to Actin (*CsACT7*), and relative expression levels were calculated using the $2^{-\Delta\Delta Ct}$ method as described previously. Primer pairs are listed in Table S2.

Motif enrichment analysis

Cis-motif enrichment analysis was performed on 2000 bp upstream sequences from the start codon (ATG) of all upregulated genes in tetraploid roots, relative to diploid roots. The analysis was conducted using the 'findMotif.pl' program from the HOMER suite, which performs both known and *de novo* motif identification and enrichment. All the analyses were carried out using findMotif.pl default parameters.

Bisulfite sequencing and data analysis

DNA extraction, bisulfite treatment, library preparation, and next-generation sequencing on the DNBseq™ platform were conducted in BGI Co. (Shenzhen, China). The BS-seq raw reads were filtered using Trimmomatic software to remove low-quality reads and adapters. Clean reads were mapped to *C. sinensis* v.3.0 or *P. trifoliata* v.1.0 genome (http://citrus.hzau.edu.cn/) using BS-Seeker2 software. Reads aligned to a unique position on the genome were retained for subsequent analysis. Differentially methylated regions (DMRs) were identified using CgmapTools with default parameter ($P \leq 0.05$, $\Delta mC \geq 0.1$). DNA methylation levels were calculated using the ratio of methylated cytosines (mC) over total cytosines (mC + nonmC) in each bin, with the absolute methylation difference ≥ 0.1, and $P \leq 0.01$ (*t*-test).

Bisulfite sequencing was applied to detect a given region's DNA methylation status. Genomic DNA from 4-month-old seedling root was extracted with the cetyl trimethylammonium bromide method. Bisulfite treatment was performed using 500 ng of DNA with the EZ DNA Methylation-Lightning Kit (D5005; Zymo Research, CA, USA). The gene regions were amplified from the 40% bisulfite-treated root DNA with primers listed in Table S2. The amplified PCR fragments were cloned into the pTOPO cloning vector (Aidlab), and at least 12 subclones were selected for each sample to conduct Sanger sequencing. Kismeth software (https://katahdin.girihlet.com/kismeth/revpage.pl) was used to obtain the percentage of methylated sites.

ATAC-seq experiment and data analysis

The method of nuclei extraction was performed as before (Liu *et al.*, 2023). After checking the nuclear integrity, the nuclei extracted (*c.* 100 000 per reaction) were incubated with the Tn5 transposase and tagmentation buffer at 37°C for 30 min (TD501-01; Vazyme Biotech, Nanjing, China). After tagmentation, the DNA is purified by the PCR purification kit (28106; Qiagen). PCR was performed to amplify the library for 9–12 cycles using the following PCR conditions: 72°C for 5 min; 98°C for 30 s; and thermocycling at 98°C for 15 s, 63°C for 30 s, and 72°C for 40 s; followed by 72°C for 5 s. After the PCR reaction, libraries were purified with AMPure beads (A63881; Beckman, IN, USA). The library was sequenced using an Illumina Novaseq platform by Annoroad Gene Technology. Paired-end read sequences were mapped using Bowtie2 (v.2.4.1) on the *C. sinensis* v.3.0 or *P. trifoliata* v.1.0 genome using the following parameters: --no-mixed --no-discordant -X 2000.

Duplicate fragments mapped on the genome were removed using PICARD MarkDuplicates. Peak calling using MACS2 (v.2.2.7) was performed with the following settings: --keep-dup all -B --SPMR --nomodel --shift -75 --extsize 150. Peak merging and identification of differential peaks were performed using DIFFBIND (v.2.14.0) and peaks with P-value < 0.05 and fold change > 1.5 were considered differentially accessible regions.

Plasmid construction and genetic transformation

The coding sequence of *CjACO1* was amplified from cDNA of diploid *C. junos* and cloned into pDONR221 and then transferred into the binary vector pK7WG2D downstream of the CaMV35S promoter (p35S). CRISPR/Cas9 genome editing vectors were produced as described previously (Zhang *et al.*, 2020). The mutation frequencies of the transgenic lines were analyzed by Hi-Tom sequencing (http://www.hi-tom.net/hi-tom/). All the primers used in this study are listed in Table S2.

The pK7WG2D-*CjACO1* and pro*YAO*-hspCas9-NOS-*CjACO1* binary vectors were introduced into the *Agrobacterium rhizogenes* strain MSU440. Diploid *C. junos* plant transformation was performed as described previously (Irigoyen *et al.*, 2020). GFP fluorescence in plants was inspected with a hand-held blue-green lamp (LUYOR-3415).

Quantification of ethylene content

Roots from 4-month-old seedlings were incubated for 1 h at 25°C to allow wound-induced ethylene content to subside and then transferred into a 5-ml Falcon tube with all the roots submerged in water. The tube was tightly sealed with a rubber cap for 12 h at 25°C. The ethylene that was emitted was subsequently measured using a gas chromatography instrument (Li *et al.*, 2020; Zheng *et al.*, 2020). Four to six biological replicates were measured.

Quantification of total flavonol content

Total flavonol content was determined following the previously reported method (Zhang *et al.*, 2022). Roots were ground to powder. Then, 1.5 ml of 80% ethanol solution was added to 0.1 g powder for 1 h of low-temperature sonication. The flavonol was extracted for 12 h at 4°C, followed by centrifugation at 2300 ***g*** for 20 min, and the liquid supernatant was retained for quantification.

Statistical analysis

Data are presented as mean values ± SD. Statistically significant differences between the two groups were determined using a two-tailed Student's *t*-test (*, $P < 0.05$; **, $P < 0.01$; ***, $P < 0.001$; ****, $P < 0.0001$). For multiple comparisons, statistically significant differences were determined using a one-way ANOVA followed by Tukey's multiple range test or Duncan's tests ($P < 0.05$) or the Kolmogorov–Smirnov test. Statistical analyses were performed with GRAPHPAD PRISM 8.0 and Microsoft EXCEL 2016.

Results

Tetraploidization enhances salt stress resilience in the *Citrus* and *Poncirus* genera

Apomictic species of *Citrus* and *Poncirus* genera can undergo spontaneous tetraploidization (Allario *et al.*, 2011; Tan *et al.*, 2017). We used this property to identify spontaneous tetraploid plants from three species, namely *Citrus junos*, *C. reticulata*, and *Poncirus trifoliata* (Fig. 1a,b). The isolated tetraploid plants exhibited larger flowers, and seeds compared with the diploid progenitors (Figs 1a, S1). Roots are the primary interface between the plant and various biotic and abiotic stresses in the soil environment. We analyzed the root morphology of tetraploid and diploid plants. Tetraploid plants across the three genotypes displayed fewer lateral roots, reduced total root length, and increased root diameter (Fig. 1c,d). We tested whether the root morphological changes in tetraploid plants can confer resilience to underground stresses. Thirty-day-old diploid *P. trifoliata* plants, exposed to 50 mM, 100 mM, and 200 mM NaCl, showed leaf injuries after 68, 37, and 15 d, respectively (Figs 2c, S2). Similar leaf injuries were observed in diploid *C. junos* and *C. reticulata* seedlings treated with 200 mM NaCl (Fig. 2a,b). By contrast, tetraploid plants displayed fewer leaves with injuries, higher Chl content, and lower hydrogen peroxide (H_2O_2) levels, pointing to reduced sensitivity to salt stress (Fig. 2a–f).

The ability to retain K^+ and limit Na^+ accumulation, thereby maintaining a higher $K^+ : Na^+$ ratio in the cytosol, is a critical parameter for salt stress resilience (Sakamoto *et al.*, 2004; Chao *et al.*, 2013). We found tetraploid *C. reticulata* and *P. trifoliata* displaying higher K^+ uptake and a higher $K^+ : Na^+$ ratio in both roots and shoots under salt stress conditions (Fig. S3). These findings align with previous studies on tetraploids in *Arabidopsis* and rice (Chao *et al.*, 2013; Wang *et al.*, 2021). Under control conditions, tetraploid *C. reticulata* and *P. trifoliata* plants also displayed higher K^+ uptake in shoots (Fig. S3).

Given the superior performance of tetraploid root systems in maintaining K^+/Na^+ homeostasis under salt stress (Fig. S3), we tested whether their use as rootstocks could also confer salt tolerance to susceptible scions. Diploid scions were grafted onto both tetraploid and diploid rootstocks and subjected, as above, to 200 mM NaCl. Across the three genotypes, plants with tetraploid rootstocks consistently exhibited fewer injured leaves, higher Chl content, and lower H_2O_2 compared with those grafted onto diploid rootstocks (Figs 2g,h, S4). These findings highlight the role of polyploidization in shaping root development to confer resilience to salt stress.

Tetraploid roots exhibit strong transcription of ethylene and ROS scavenging genes

To explore the molecular basis driving resilience to salt stress following genome doubling, we analyzed the roots transcriptome of tetraploid and diploid plants under control and salt stress conditions. Roots were sampled at 24 h post treatment, in three biological replicates, at a stage where the early salt-responsive genes,

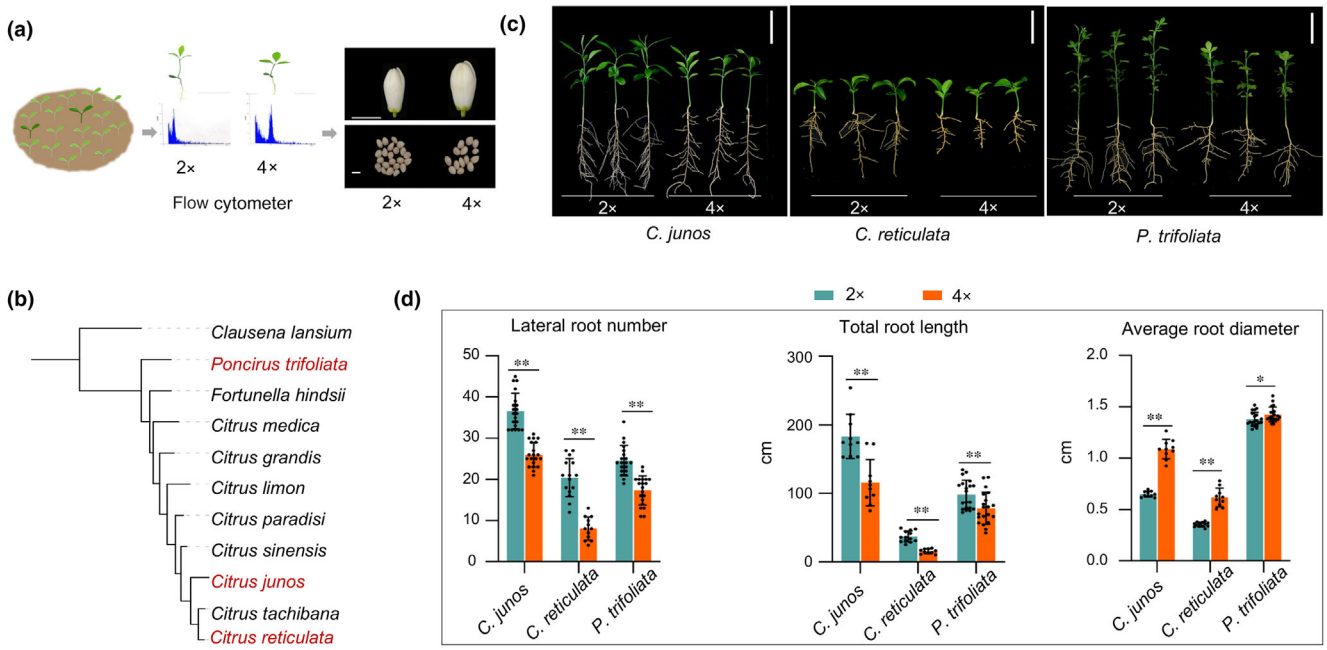

Fig. 1 Tetraploidization leads to a compacted root system in the *Citrus* and *Poncirus* genera. (a) Schematic diagram for identification of spontaneous tetraploids using flow cytometric analysis. Seedlings with greener and larger leaves, which have a higher probability of being tetraploids (4×), from diploid (2×) apomictic citrus genotypes, are selected for analysis. Flowers and seeds of 4× and 2× *Citrus junos* are shown. Bars, 1 cm. (b) Phylogenetic tree of representative citrus species. Three genotypes highlighted in red are used in this study. A phylogenetic tree is constructed using the maximum likelihood method. Single-nucleotide polymorphisms (SNPs) in the regions of conserved single-copy genes from 11 representative accessions within the Rutaceae family are used. (c) Comparison of root morphology between 4× and 2× plants. Bars, 1 cm. (d) Statistical analysis of root parameters in 4× and 2× plants. Bar plots represent mean ± SD (n = 10–20). Statistically significant difference is tested by Student's t-test: *, $P < 0.05$; **, $P < 0.01$.

STZ1, *WRKY33*, and *WRKY40* (Sakamoto *et al.*, 2004; Datta *et al.*, 2015; Dai *et al.*, 2018) are highly expressed (Figs S5, S6; Table S3).

Under salt stress, we found 3585, 2805, and 4349 genes upregulated (> 1.5-fold, false discovery rate (FDR) < 0.05), and 3012, 1537, and 3782 genes downregulated (> 1.5-fold, FDR < 0.05) in the roots of tetraploid *C. junos*, *C. reticulata*, and *P. trifoliata*, compared with their diploid progenitors, respectively (Fig. 3a; Tables S4–S6). Despite the divergence of the investigated genotypes, we found under salt treatment, 20–30% of upregulated genes (847 genes) and 18–28% of downregulated genes (245 genes) were common across all the three tetraploid genotypes (Fig. 3b; Table S7). Under control conditions, despite comparable numbers of differentially expressed genes (Fig. S6; Tables S8–S10), only 5–8% (55 genes) of upregulated, and 3–10% (64 genes) of downregulated genes, were common (Fig. S6; Table S11).

Gene Ontology analysis on 847 shared upregulated genes revealed enrichment for GO terms related to response to stimuli (295 genes) and stress (188 genes) (Fig. 3c). Among the 188 stress response genes, six encode glutathione S-transferase (GSTUs), three encode peroxidase superfamily proteins (PRX52, PER16, and PRX25), one encodes a cupredoxin superfamily protein (SC2), and three encode alternative oxidase (AOX1a, AOX1d-1, and AOX1d-2) (Fig. 3d), key proteins implicated in the modulation of ROS homeostasis under salt stress (Smirnoff & Arnaud, 2019; Sweetman *et al.*, 2019; Gong *et al.*, 2020; Sun *et al.*, 2024). Consistent with this, we found under salt stress conditions, roots of tetraploid plants significantly accumulating less H_2O_2 (Fig. 3e). Under control conditions, we also found an enrichment of stress response genes, pointing to a priming for stress resilience (Fig. S6). Alongside stress response genes, we found an enrichment in GO terms related to hormones with the largest number involved in the ethylene pathway, followed by jasmonic acid (JA) and abscisic acid (ABA) (Fig. 3c,d). Specifically, 20 genes were involved in ethylene biosynthesis and signaling, including three ethylene biosynthesis-related genes: *ACO1*, *ACS1*, and *ACS6*, along with 15 ethylene response factors (*ERFs*) (Fig. 3d).

We also investigated the downstream genes regulated by these hormones by examining motif enrichment in the promoters of the 874 upregulated genes. The top three most enriched motifs were WRKY (TTGAC(C/T)), CAMTA1 calmodulin-binding transcription activator 1 (CAMTA1) (CGCGT), and the ERF-binding motif (GCC box) (Fig. S7). Approximately 30% of the upregulated genes contained the GCC box motif in their promoters ($P < 10^{-12}$), suggesting that genes responsive to ethylene play a major role in the salt stress resilience of tetraploids.

Transcriptome analysis revealed strong upregulation of genes related to ethylene biosynthesis and signaling genes, emphasizing ethylene's role in the salt stress resilience of tetraploids. Ethylene was also known to influence root architecture (Smalle & Van Der Straeten, 1997; Negi *et al.*, 2008), promoting thicker roots with fewer branches – traits observed in tetraploids. These

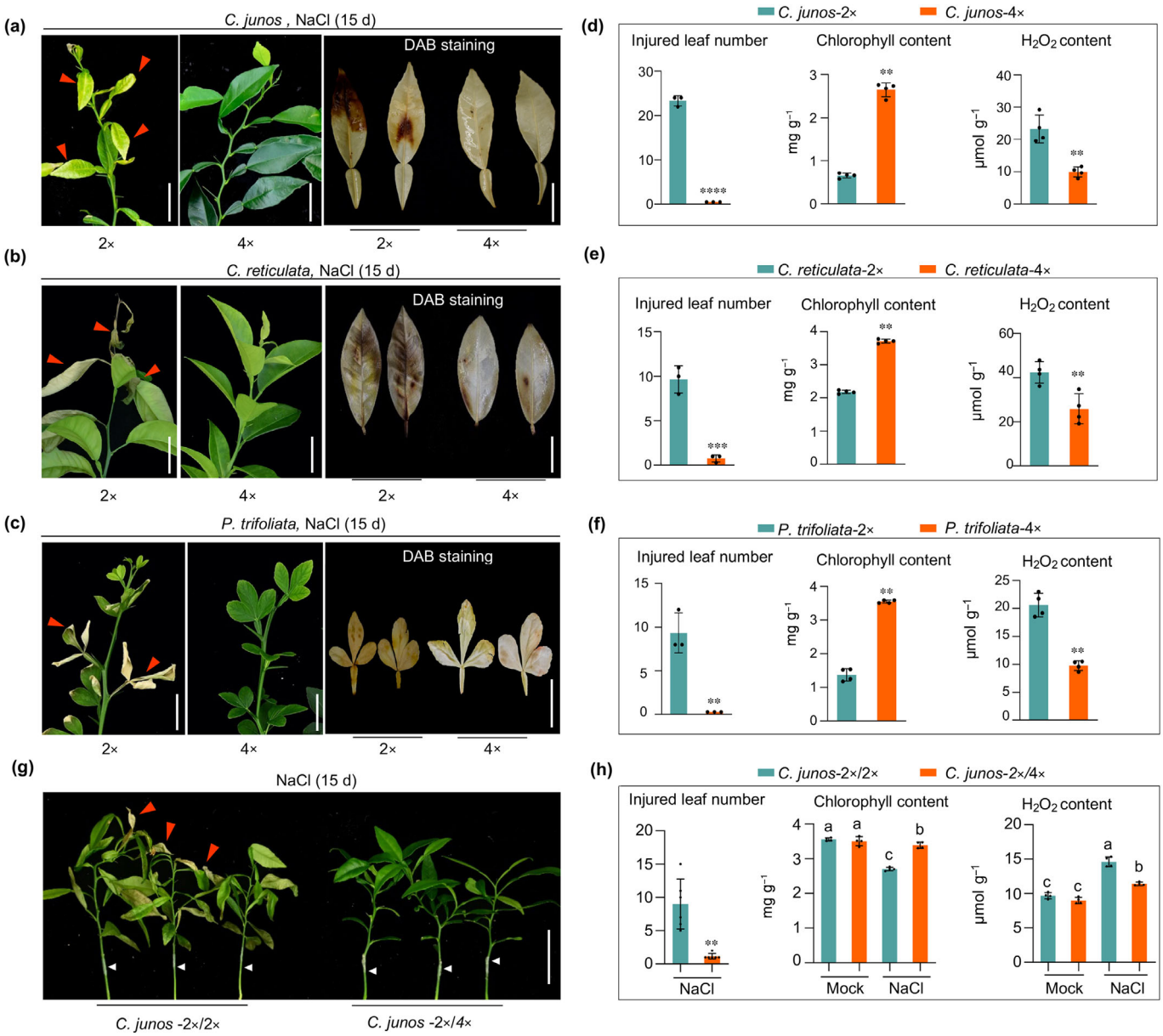

Fig. 2 Tetraploidization enhances salt stress resilience in the *Citrus* and *Poncirus* genera. (a–c) Leaf injuries and reactive oxygen species (ROS) staining of tetraploids (4×) and diploid (2×) plants from three genotypes treated with NaCl. Four-month-old plants are treated with 200 mM NaCl for 15 d. Red arrows indicate injured leaves. Leaves stained with DAB are used to assess the accumulation of H_2O_2. Bar, 2 cm. (d–f) Statistical analysis of injured leaf number, leaf Chl, and H_2O_2 content in NaCl-treated 2× and 4× plants. Bars indicate mean values ± SD (n = 3–4). Statistically significant differences are determined using a Student's t-test: **, $P < 0.01$; ***, $P < 0.01$; ****, $P < 0.0001$. (g) Leaf injuries of grafted 2×/2× (scion/rootstock) and 2×/4× (scion/rootstock) *Citrus junos* plants. One-month-old plants are used for grafting, and after 1 month of recovery, the grafted plants are subjected to a 15-d treatment with 200 mM NaCl. Grafted plants of other genotypes are shown in Supporting Information Fig. S4. Red and white arrows indicate injured leaves and grafting interface, respectively. Bar, 5 cm. (h) Statistical analysis of injured leaf number, leaf Chl, and H_2O_2 content in grafted plants treated with NaCl. Leaves from three to five plants are pooled to form a single replicate. Bar plots represent mean ± SD (n = 4–6). Statistically significant difference is tested by Student's t-test (**, $P < 0.01$) or ANOVA (different letters). All data above are collected in 2021.

findings prompted further investigation into ethylene's role in tetraploidization-mediated stress resilience, rather than focusing on other hormones.

Ethylene biosynthesis genes are highly tuned to control ethylene signaling (Booker & DeLong, 2015). We identified *ACO1* as the most highly upregulated biosynthesis gene following tetraploidization (Tables S7, S11). The citrus genome contains nine putative *ACO* genes (Fig. S8), among which only *ACO1* and *ACO5* were highly expressed in the roots (Fig. S8). *ACO1* showed the highest expression in the roots compared with other plant tissues (Fig. S8), indicating its significant role in ethylene production in roots. Notably, we found that *ACO1* was highly

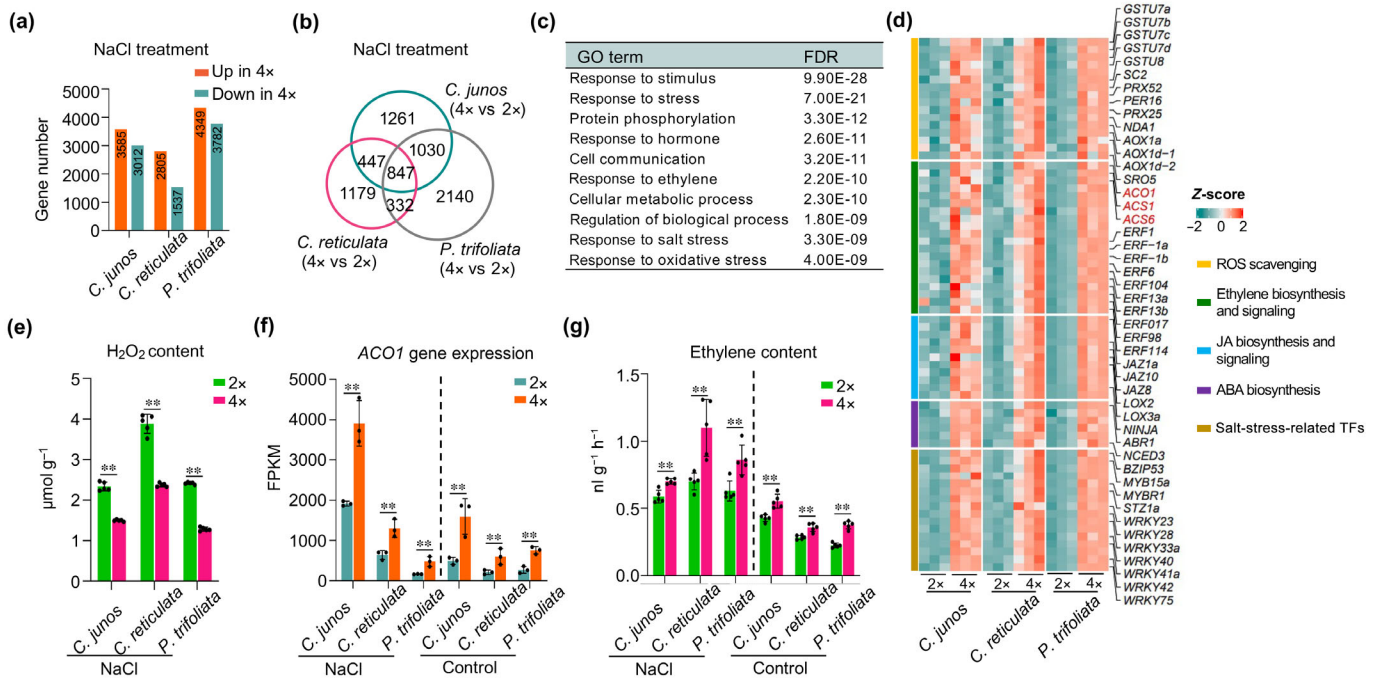

Fig. 3 Tetraploid roots exhibit stronger transcription of ethylene and reactive oxygen species (ROS) scavenging genes. (a) Number of differentially expressed gene in roots between tetraploids (4×) and diploid (2×) plants in the *Citrus* and *Poncirus* genera under NaCl treatment. Entire roots after 24 h of NaCl treatment (200 mM) are used for transcriptomic analysis. Genes with false discovery rate (FDR) < 0.05 and fold change (FC) > 1.5 are considered differentially expressed. (b) Venn diagrams showing upregulated genes in 4× roots relative to 2× roots overlapping among three genotypes under NaCl treatment. (c) Gene Ontology (GO) enrichment analysis of 847 upregulated genes in 4× roots relative to 2× roots shared among three genotypes under NaCl treatment. The top 10 GO terms are shown. False discovery rate (FDR) is calculated using Fisher's test. (d) Heatmap showing expression levels of stress-related pathway genes between 4× and 2× plants under NaCl treatment. For each gene, the fragments per kilobase of transcript per million mapped reads (FPKM) value is normalized by the *Z*-score (FPKM minus mean over SD). (e) Statistical analysis of H_2O_2 content in roots of 4× and 2× plants under NaCl treatment. Leaves from three to five plants are pooled to form a single replicate. Bar plots indicate mean values ± SD (n = 5). Statistically significant differences are determined using a Student's *t*-test: **, $P < 0.01$. (f) Expression levels of the ethylene biosynthesis gene *ACO1* between 4× and 2× roots among three genotypes under NaCl treatment and control conditions. Expression data are obtained from entire root transcriptomic analysis. Data represent mean values ± SD (n = 3, **, $P < 0.01$, Student's *t*-test). (g) Statistical analysis of ethylene content in the roots of 4× and 2× plants under NaCl treatment and control conditions. Data represent mean values ± SD (n = 5, **, $P < 0.01$, Student's *t*-test).

upregulated in tetraploid roots under both salt stress and control conditions (Figs 3f, S6), pointing to a central role in maintaining basal and stress-induced ethylene levels.

To test whether ethylene production is enhanced in tetraploid plants, we measured ethylene levels in roots under both control and salt stress conditions. As expected, tetraploid roots had significantly higher ethylene levels under both conditions (Fig. 3g).

Ethylene treatment in diploids replicates the root phenotype and salt stress resilience in tetraploids

Increased ethylene production is known to inhibit primary root elongation by affecting both cell division and cell elongation processes, and it also reduces the formation of lateral roots (Ivanchenko *et al.*, 2008; Negi *et al.*, 2008; Lewis *et al.*, 2011). As tetraploid plants are characterized by shorter, thicker primary roots with a reduced number of lateral roots, we hypothesized that elevated ethylene levels in tetraploids could be responsible for driving these changes. To explore this, we treated diploid seedlings with ACC, an ethylene precursor, to artificially elevate ethylene levels. After 45 d of treatment with 20 μM ACC, the plants exhibited thicker, shorter primary roots with fewer lateral roots, closely resembling the root architecture seen in tetraploid plants (Figs 1c,d, S9). Similar root modifications were also observed at lower ACC concentrations (10 and 5 μM; Fig. S9).

To determine whether the ethylene-induced root phenotype also contributes to enhanced salt stress resilience, we grew ACC-treated diploid plants under salt stress conditions. Compared with the control plants, the ACC-treated plants demonstrated fewer wilted and chlorotic leaves, maintained higher Chl content, and exhibited lower levels of H_2O_2, indicative of reduced oxidative stress (Fig. S9). These findings suggest that exogenous ethylene treatment mimics the effects of genome doubling on root architecture and improves salt stress resilience.

Analysis of *ACO1* overexpression and knockout lines under salt stress

The increased expression of the *ACO1* gene in tetraploid plants, along with the results from the ethylene treatment experiment,

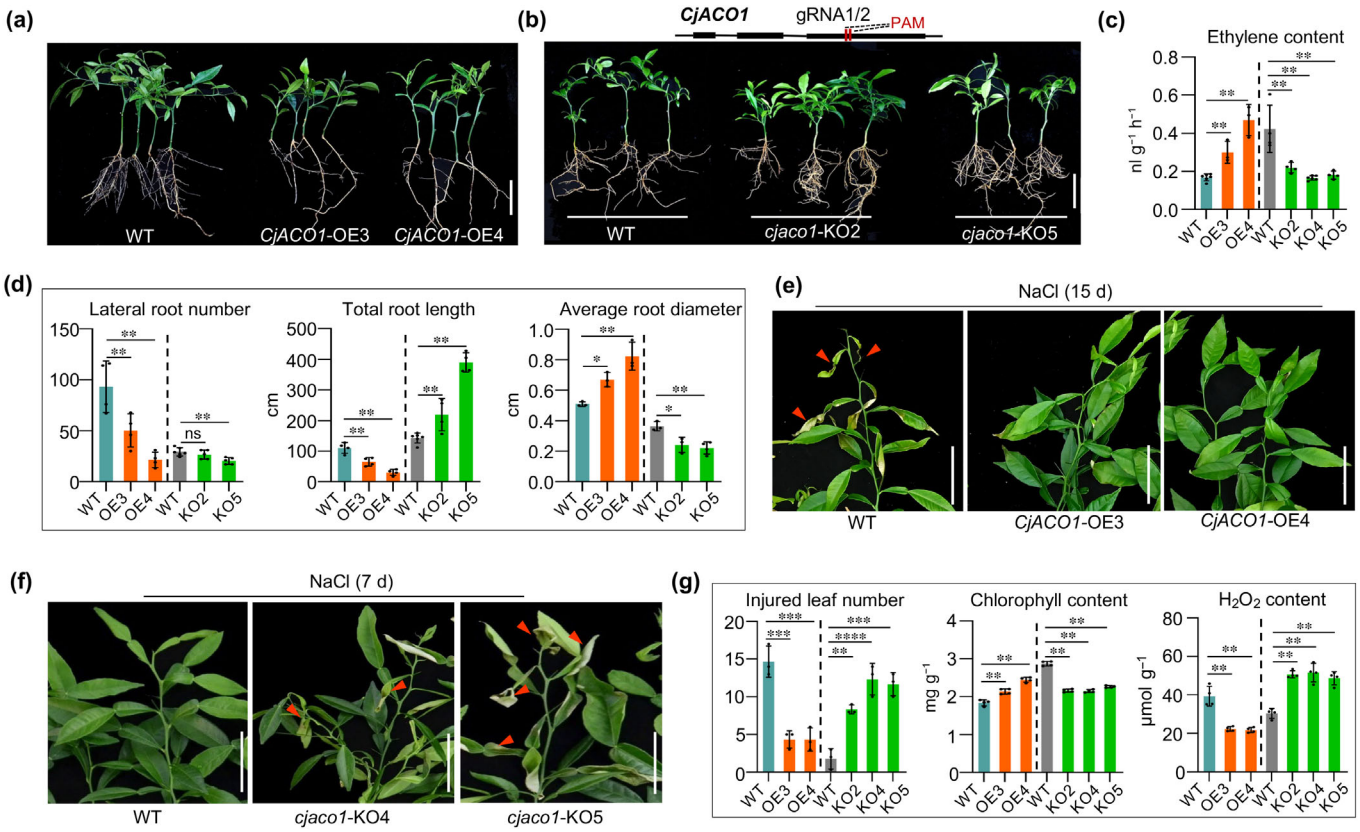

Fig. 4 Transgenic manipulation of *ACO1* replicates the root phenotype and salt stress resilience observed in tetraploids. (a) Plant phenotypes of wild-type (WT) and *CjACO1* root-specific overexpression (OE) lines. Diploid *Citrus junos* plants are used for *Agrobacterium rhizogenes-mediated* transformation. Two-month-old plants are shown. Bar, 5 cm. (b) Plant phenotypes of WT and *CjACO1* knockout (KO) lines. Two gRNA target sites are indicated by red vertical lines (upper). Two-month-old plants are shown. Bar, 5 cm. (c) Statistical analysis of ethylene content in the roots of WT, *CjACO1*-OE and *CjACO1*-KO plants. Bar plots indicate mean values ± SD (n = 4–6). Statistically significant difference is tested by Student's t-test: **, $P < 0.01$. (d) Statistical analysis of root parameters in WT, *CjACO1*-OE, and *CjACO1*-KO plants. Bar plots represent mean ± SD (n = 3–6). Statistically significant difference is tested by Student's t-test: *, $P < 0.05$; **, $P < 0.01$; ns, no significant difference. (e, f) Leaf injuries of WT, *CjACO1*-OE (e), and *CjACO1*-KO (f) plants treated with NaCl. Four-month-old plants are treated with 200 mM NaCl for 15 d (e) or 7 d (f). Red arrows indicate injured leaves. Bars, 5 cm. (g) Statistical analysis of injured leaf number, leaf Chl, and H_2O_2 content in WT, *CjACO1*-OE, and *CjACO1*-KO plants. Bar plots represent mean ± SD (n = 4). Statistically significant difference is tested by Student's t-test: **, $P < 0.01$; ***, $P < 0.001$; ****, $P < 0.0001$.

underscores the pivotal role of *ACO1* in enhancing salt stress resilience following genome doubling (Figs 3f, S9). To functionally validate this role, we generated both *ACO1* overexpression and knockout (KO) lines in diploid citrus plants. The overexpression lines were developed by inducing root-specific expression of *ACO1* using Agrobacterium-mediated hairy root transformation (Figs 4a, S10). The *ACO1* KO lines were created using the CRISPR-Cas9 gene-editing tool (Figs 4b, S10). In total, four *ACO1* overexpression lines and five KO mutants were produced, including two homozygous lines (KO4 and KO5) and one heterozygous line (KO2) with an 81.3% allele mutation rate (Figs 4b, S10). As expected, the *ACO1* overexpression (*CjACO1*-OE) lines displayed significantly higher ethylene levels in the roots, while the *ACO1* KO lines showed a marked reduction in ethylene content (Fig. 4c). Phenotypically, the *CjACO1*-OE lines developed fewer lateral roots, shorter total root lengths, and increased root diameter, closely mimicking the root architecture observed in tetraploids, and in diploid plants treated with ethylene (Figs 1c,d, 4d, S9). Conversely, the KO2 and KO5 lines showed longer and thinner roots, further confirming *ACO1*'s effect on root development (Fig. 4d). To further explore whether the enhanced salt stress resilience of tetraploid plants is driven by upregulated *ACO1* expression, we subjected both *CjACO1*-OE and KO plants to 200 mM NaCl salt stress, for 14 and 7 d, respectively. The *CjACO1*-OE lines showed significantly improved salt tolerance, evidenced by fewer wilted and chlorotic leaves, higher Chl content, and lower H_2O_2 levels compared with nontransformed control plants (Fig. 4e,g). By contrast, the KO lines were severely affected by the salt stress, exhibiting extensive wilting and bleaching of the shoots (Fig. 4f,g). The KO lines also accumulated much lower levels of Chl and higher levels of H_2O_2 than the nontransformant control plants (Fig. 4g).

These results strongly validate the central role of the regulation of *ACO1* expression in modulating root architecture and salt stress resilience in tetraploid plants.

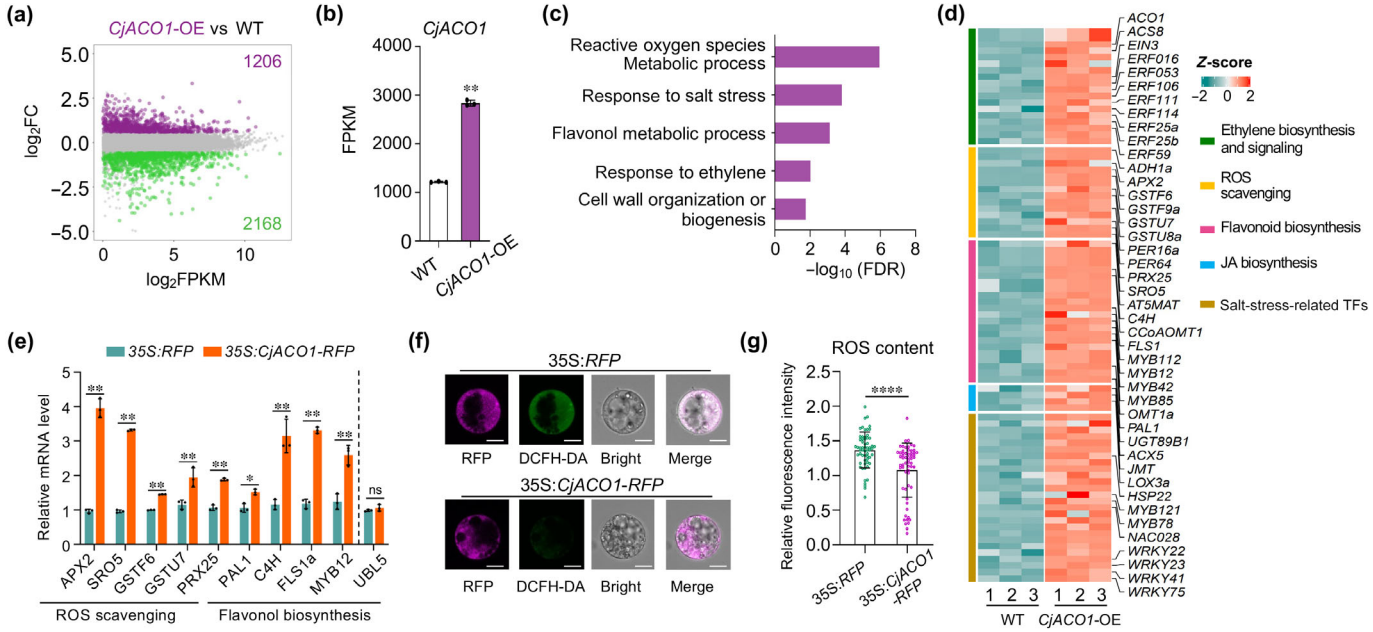

Fig. 5 Increased *ACO1* expression results in enhanced reactive oxygen species (ROS) scavenging and flavonol biosynthesis in root. (a) Average read count plots of gene expression changes in roots of *CjACO1* overexpression (OE) lines vs wild-type (WT). Cj, *Citrus junos*. The *x*-axis represents average gene expression level (fragments per kilobase of transcript per million mapped reads (FPKM)), and the *y*-axis represents $\log_2$FC (*CjACO1*-OE/WT). FC, fold change. Significantly (false discovery rate (FDR) < 0.05 and 1.5-FC) upregulated and downregulated differentially expressed genes are indicated. (b) FPKM values of *ACO1* in *CjACO1*-OE and WT roots. FPKM values are extracted from root transcriptomic data. Bar plots represent mean ± SD (n = 3). **, P < 0.01 (Student's *t*-test). (c) Gene Ontology (GO) enrichment analysis of upregulated genes in *CjACO1*-OE plants. The top five GO terms are shown. FDR is calculated using Fisher's test. (d) Heatmap showing expression levels of genes from GO terms in (c). Heatmap presents scaled values of normalized FPKM from transcriptomic data. Typical genes in the corresponding term are indicated on the right. For each gene, the FPKM value is normalized by the *Z*-score (FPKM minus mean over SD). (e) Quantitative reverse transcription polymerase chain reaction analysis of gene expression in citrus leaf protoplasts expressing *CjACO1-RFP* or *RFP*. *CsUBL5* and *CsACT7* are control genes. Bar plots represent mean ± SD (n = 3). *, P < 0.05; **, P < 0.01; ns, no significant difference (Student's *t*-test). (f) DCFH-DA (2′,7′-dichlorodihydrofluorescein diacetate) staining of citrus protoplasts expressing *CjACO1-RFP* or *RFP*. Bars, 10 μm. A total of 60 protoplasts are observed. (g) Relative DCFH-DA fluorescence intensity in citrus protoplasts expressing *CjACO1-RFP* or *RFP*. Fluorescence (F488/F552 nm) is quantified using ImageJ. Bar plots represent mean ± SD (n = 60). ****, P < 0.0001 (Kolmogorov–Smirnov test).

Increased *ACO1* expression results in enhanced ROS scavenging and flavonol biosynthesis in root

Considering that enhanced salt tolerance is linked to elevated *ACO1* expression, and that knocking out *ACO1* disrupts this resilience, we conducted a detailed analysis of the root transcriptomes of *CjACO1* overexpression lines (*CjACO1*-OE) (Fig. S11; Table S3). We identified 1206 genes that were significantly upregulated (> 1.5-fold, FDR < 0.05), and 2168 genes that were significantly downregulated (> 1.5-fold, FDR < 0.05), in the roots of *CjACO1*-OE, compared with the untransformed control line (Fig. 5a,b; Table S12). Similar to the root transcriptomes of tetraploids, the upregulated genes in *CjACO1*-OE roots were enriched in pathways associated with ethylene biosynthesis and signaling, ROS scavenging, and metabolic processes of phenylpropanoids and flavonoids. This includes 34 genes involved in ethylene biosynthesis and signaling, such as *ACS8*, *EIN3*, and 10 *ERFs* (Fig. 5c,d). Additionally, several ROS scavenging-related genes, such as *ASCORBATE PEROXIDASE 2* (*APX2*), *SIMILAR TO RCD ONE 5* (*SRO5*), and *ALTERNATIVE NAD(P)H DEHYDROGENASE 1* (*NDA1*), were also upregulated (Fig. 5d). These genes are vital for mitigating oxidative stress under abiotic stress conditions, as documented in previous studies (Dai *et al.*, 2018; Sweetman *et al.*, 2019; Zhu *et al.*, 2020). Key enzymes that regulate phenylpropanoid and flavonoid biosynthesis (Liu *et al.*, 2015), including PHENYLALANINE AMMONIA LYASE (PAL1), CINNAMATE 4-HYDROXYLASE (C4H), FLAVONOL SYNTHASE (FLS), and the transcription factor MYB12 (a master regulator of the R2R3-MYB family), were also upregulated in *CjACO1*-OE roots (Fig. 5d). qPCR analysis confirmed that these genes were also induced in plants treated with ACC (Fig. S11). Consistent with these transcriptomic changes, both *CjACO1*-OE and ACC-treated plants exhibited lower H_2O_2 levels and higher flavonol concentrations in their roots (Fig. S11). The increased flavonol biosynthesis is likely a key factor contributing to the enhanced salt stress resilience, observed in *CjACO1*-OE, ACC-treated, and tetraploid plants, as flavonols are known substrates for peroxidases involved in ROS scavenging, particularly of H_2O_2 (Gayomba & Muday, 2020).

To further validate the role of *ACO1* in influencing ROS scavenging and flavonol biosynthesis, we transiently expressed *CjACO1* fused to a red fluorescent protein (RFP) reporter in citrus

leaf protoplasts. Subsequent qPCR analysis and ROS staining assays revealed that protoplasts expressing *CjACO1-RFP* exhibited activation of both ROS scavenging and flavonol biosynthesis-related genes, while the control protoplasts expressing RFP alone showed no significant changes (Fig. 5e). Furthermore, protoplasts expressing *CjACO1-RFP* displayed significantly lower ROS levels compared with the controls (Fig. 5f,g). These findings demonstrate that elevated *ACO1* expression results in enhanced ROS scavenging and promotes flavonol biosynthesis, thereby contributing to improved stress tolerance.

Interestingly, several JA biosynthesis genes were also upregulated in the roots of *CjACO1*-OE plants (Fig. 5d) as well as in tetraploid plants (Fig. 3d), suggesting that ethylene signaling may play a role in promoting JA biosynthesis. Given that ethylene and JA interact through complex crosstalk networks in stress responses (Zhu *et al.*, 2011; Hu *et al.*, 2021), the upregulation of genes involved in ROS scavenging and flavonol biosynthesis in *CjACO1*-OE plants may also result from hormone crosstalk.

In summary, our findings highlight that increasing ethylene production in roots stimulates the transcription of genes involved in ROS scavenging, flavonol biosynthesis, and JA biosynthesis, all of which contribute to the plant's resilience to salt stress. These results also underscore the central role of *ACO1* expression in coordinating salt stress tolerance, particularly in tetraploid plants.

Tetraploidization results in hypomethylation and enhanced chromatin accessibility of *ACO1*

To explore how *ACO1* expression is regulated in the roots of tetraploid plants, we conducted a comprehensive analysis of genome-wide DNA methylation and chromatin accessibility. DNA methylation analysis was performed using whole-genome bisulfite sequencing (BS-seq) on the roots of tetraploids and their diploid progenitors under control conditions (Table S3). The Pearson correlation coefficients among the three biological replicates exceeded 0.98, indicating high reproducibility of the methylome data (Fig. S12). To identify variations in DNA methylation, we looked for DMRs between tetraploid and diploid plants ($P \leq 0.05$, $\Delta mC \geq 0.1$). Across the genomes of tetraploid *C. junos*, *C. reticulata*, and *P. trifoliata*, we found 8194, 10 901, and 3165 hypermethylated DMRs and 6560, 7518, and 3165 hypomethylated DMRs, respectively (Tables S13–S15). Interestingly, no significant changes in CHG and CHH DNA methylation were observed in the *ACO1* promoter and gene body between tetraploid and diploid plants (Fig. S13). However, we identified hypomethylated DMRs in the CG context within the gene body of *ACO1* (Fig. S14).

To further confirm the presence of these CG hypo-DMRs in the *ACO1* gene body, we employed bisulfite sequencing-PCR (BSP). We specifically focused on the region containing the identified CG hypo-DMR, which is located 3′ downstream of the start codon, spanning 597 to 1268 bp. This region exhibited significantly reduced CG methylation in tetraploid plants compared with diploid plants across all three genotypes, validating our genome-wide methylation analysis (Fig. S14).

We also assessed chromatin accessibility using ATAC-seq analysis on root chromatins from two tetraploid genotypes, *C. reticulata* and *P. trifoliata*, as well as their diploid progenitors under control conditions (Table S3). Genome-wide chromatin accessibility patterns in tetraploid and diploid roots were strikingly similar, showing enrichment at transcription start and termination sites (Figs 6a,b, S15). Nevertheless, *ACO1* showed significantly increased chromatin accessibility at the transcription start site, corresponding to its upregulated expression under both control and stress conditions in tetraploid plants (Fig. 6c; Tables S16, S17). This supports our finding that tetraploid roots have a stronger transcriptional response to early-stage salt stress compared with diploid roots (Fig. 3a,d). Alongside *ACO1*, other ethylene biosynthesis and signaling genes, such as *ACS6*, *ERF1*, *ERF104*, and *ERF017*, as well as the flavonol biosynthesis genes *FLS1* and *PAL1*, and the ROS scavenging gene *AOX1d*, which were upregulated in tetraploid roots under salt treatment, also showed greater chromatin accessibility in tetraploid *C. reticulata* and *P. trifoliata* (Figs 3d, S16). Collectively, our findings emphasize that genome doubling drives hypomethylation and chromatin remodeling of upregulated genes, such as *ACO1*, which is essential for activating pathways that enhance resilience to salt stress.

Discussion

Throughout evolution, most flowering plants have undergone one or more independent genome-doubling events, underscoring polyploidization as a key driver in the emergence of new species and adaptation to changing environments (Chen, 2007). However, it remains unclear whether genome doubling alone is sufficient to mediate some of these adaptations, or if subsequent mutations leading to new gene functions are necessary to confer genetic advantages. In this study, we leveraged the apomictic reproductive system of citrus species within the Rutaceae family, which can spontaneously undergo tetraploidization, to generate genetically identical clones differing only in ploidy levels, and comparative phenotyping to the diploid progenitors for resilience. Our findings reveal that tetraploid clones exhibit a stronger root system and improved functionality under salt stress, phenotypes that are likely orchestrated by chromatin remodeling of the *ACO1* gene.

Our analysis also indicates that the elevated expression of *ACO1* in tetraploid plants does not stem from changes in promoter DNA methylation in the CHG and CHH contexts, as no significant alterations were observed (Fig. S13). Instead, we detected a decrease in CG DNA methylation within the *ACO1* gene body across all tetraploid plants, which correlates with *ACO1* expression upregulation (Fig. S14). Although the precise function of intragenic methylation remains unclear, similar decreases in gene body methylation have been observed in newly formed tetraploid grapevines (Zou *et al.*, 2020), suggesting a possible link between reduced methylation and increased gene expression.

Significantly, we found a marked increase in chromatin accessibility at the transcription start site of *ACO1* in tetraploid plants (Fig. 6c). This increase in accessibility likely facilitates the

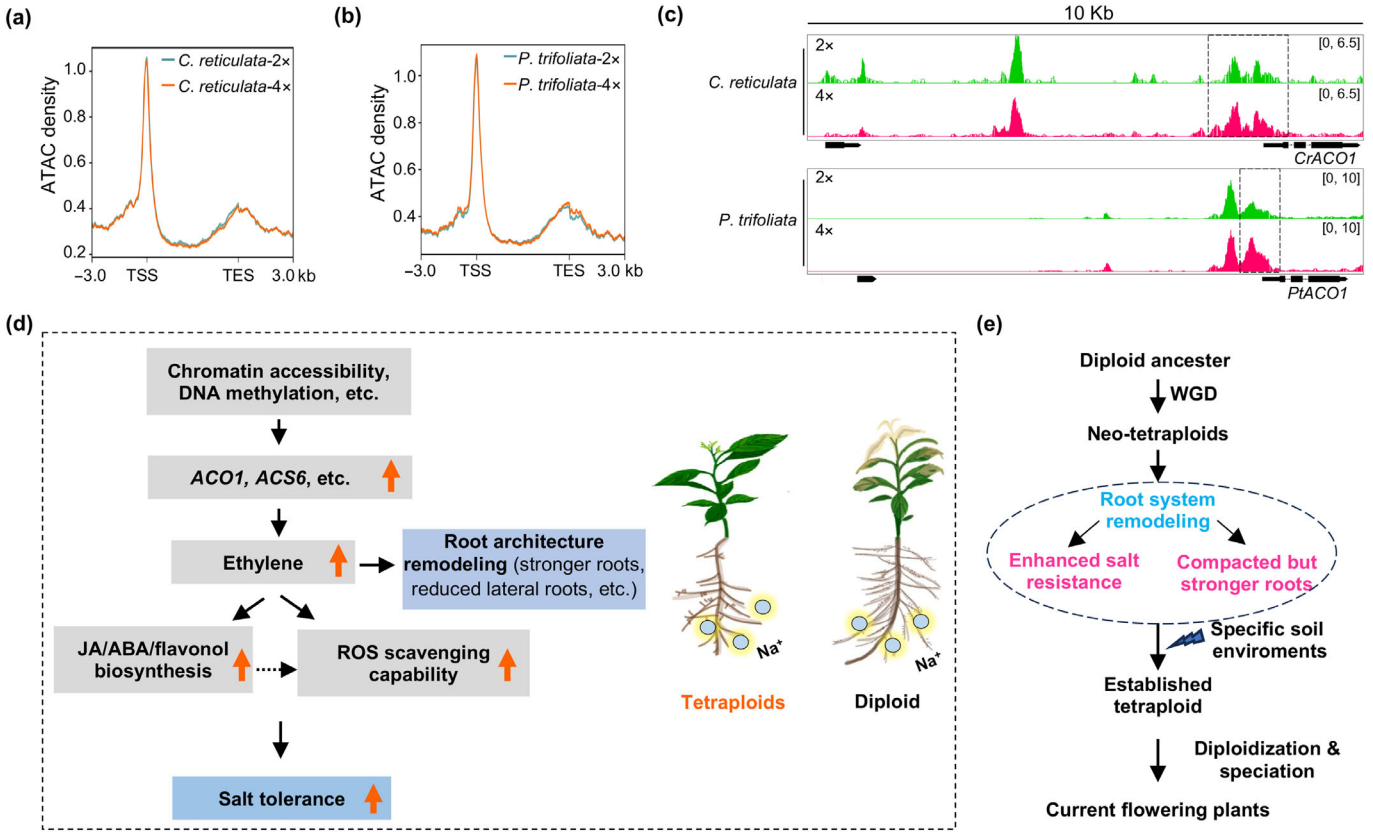

Fig. 6 Proposed working model illustrating distinct root architecture and enhanced salt stress resistance in tetraploids. (a, b) Genome-wide distribution of ATAC-seq peaks detected in tetraploids (4×) and diploid (2×) roots of *Citrus reticulata* (a) and *Poncirus trifoliata* (b). Entire roots under control conditions are used in ATAC-seq. Window size: gene body ±3.0 kb. (c) ATAC-seq profiles at the *ACO1* gene locus. Dotted box indicates differentially accessible peaks between 4× and 2× roots. Black arrow indicates gene transcriptional direction. (d) Molecular working model depicting the distinct root architecture and enhanced salt tolerance in tetraploids. Tetraploid roots exhibit elevated ethylene levels due to increased expression of *ACO1*, *ACS6*, and other related genes, consequently influencing the distinctive root architecture observed in tetraploid plants. Meanwhile, higher ethylene levels stimulate the transcription of genes associated with jasmonic acid (JA), abscisic acid (ABA), and flavonol biosynthesis, as well as genes involved in ROS scavenging. This cascade enhances the root's capacity for ROS scavenging, ultimately contributing to the enhanced salt tolerance observed in tetraploids. Solid lines represent pathways elucidated in this study, while dashed lines indicate pathways requiring further investigation. Black arrows denote positive regulation. Orange arrows indicate enhancement in tetraploids. (e) Significance of root system remodeling by genome doubling in flowering plant evolution. After whole-genome doubling, the root system of the neo-tetraploid is remodeled, resulting in stronger roots and enhanced salt tolerance, which facilitated neo-tetraploid survival and establishment in specific soil environments. Subsequent diploidization and speciation led to the evolution of the current flowering plants. The lightning bolt symbol represents 'selection pressure from specific soil environments'.

elevated expression of *ACO1*, which in turn drives higher ethylene production in tetraploid roots, contributing significantly to their enhanced salt tolerance (Fig. 6d). Supporting evidence includes experiments where overexpressing *ACO1* in diploid plants' roots boosted ethylene production and activated resilience metabolic pathways similar to those observed in tetraploids (Figs 4c, 5d). Additionally, pretreating the roots of diploid plants with ACC also enhanced salt tolerance (Fig. S9), demonstrating that ethylene plays a critical role in the plant's stress response. In addition to the upregulation of ethylene-related genes, genes related to other hormones, such as ABA and JA, are also upregulated in tetraploids (Fig. 3d). This suggests potential crosstalk between multiple hormones, which may collectively contribute to the increased salt tolerance in tetraploids.

Under normal conditions, tetraploid plants also exhibit increased chromatin accessibility in ROS scavenging genes, including those encoding alternative oxidase, GSTUs, and flavonol biosynthesis enzymes, that play a crucial role in protecting plants from oxidative stress (Sweetman *et al.*, 2019; Gayomba & Muday, 2020; Zhu *et al.*, 2020). These genes help neutralize harmful ROS, which can accumulate under salinity stress (Dai *et al.*, 2018). Alternative oxidases function as a terminal oxidase in the mitochondrial electron transport chain, preventing over-reduction of components and reducing ROS formation under plant stress conditions (Maxwell *et al.*, 1999), while GSTUs detoxify harmful compounds by conjugating them with glutathione (Sun *et al.*, 2024). Flavonol biosynthesis, on the contrary, produces flavonoids that act as antioxidants, further enhancing the plant's defense system (Gayomba & Muday, 2020). This increased accessibility allows transcriptional regulators to more readily bind and activate these genes when the plants are exposed to salt stress, enabling a quicker and more robust

transcriptional response compared with diploid counterparts. While transcriptome and chromatin accessibility analyses have provided key insights, they offer only a partial understanding of the mechanisms through which chromosome doubling enhances abiotic stress tolerance. Other factors, such as histone modifications (Ding & Chen, 2018), chromatin organization (Zhang *et al.*, 2019), and post-translational modifications (Zhang *et al.*, 2022), likely play significant roles as well. Analyzing these aspects presents promising directions for future research.

Genome doubling during evolution and adaptation often results in multiple gene paralogs, though most duplicated genes are eventually lost (Innan & Kondrashov, 2010). Some are retained through neofunctionalization, subfunctionalization, or beneficial increases in gene dosage (Panchy *et al.*, 2016). In this context, *ACO* genes have multiple homologs in most plants (e.g. 5 *ACOs* in *Arabidopsis thaliana* and 9 in the *C. sinensis* genome). Among these, *ACO1* is the most highly expressed in citrus roots, and its overexpression leads to higher ethylene production and enhanced salt tolerance. Conversely, the loss of *ACO1* function results in lower ethylene production and increased salt sensitivity, underscoring its key role in root resilience. We found that the expression of the other *ACO* genes does not change with genome doubling (Tables S4–S6), indicating that they do not contribute to the salt stress resilience observed in tetraploid plants.

The elevated expression of *ACO1* in tetraploid genotypes results in thicker roots with reduced lateral branching (Fig. 1c,d), which may improve soil penetration, promote deeper rooting, and reduce the metabolic costs associated with root construction (Zhan *et al.*, 2015; Klein *et al.*, 2020; Lynch, 2022). These structural changes in the roots likely contribute to the increased survival and adaptability of newly formed polyploid plants in specific soil conditions (Fig. 6e). Moreover, increased *ACO1* expression or ethylene biosynthesis may also promote early fruit maturation (Wang *et al.*, 2019) and seed germination (Linkies *et al.*, 2009), aiding in seed dispersal and boosting the reproductive capacity of newly formed polyploids.

Elevated *ACO1* expression has also been observed in colchicine-induced tetraploid grapevines (Zou *et al.*, 2020) and in tetraploid *C. junos* leaves (Tan *et al.*, 2015), suggesting that gene dosage significantly influences *ACO1* function. Interestingly, the *constitutive triple response* 1 (*ctr1*) mutant of *Arabidopsis*, which exhibits increased ethylene signaling, shows higher polyploidy levels in hypocotyls (Yoshizumi *et al.*, 2006), further highlighting the complex interplay between polyploidy and ethylene signaling in plant adaptation and evolution.

The permissive chromatin environment for *ACO1* expression in tetraploid roots likely results from a combination of interrelated mechanisms. Genome doubling may lead to a redistribution of DNA methylation patterns, as observed in tetraploids (Wang *et al.*, 2021; Gao *et al.*, 2024). Changes in noncoding RNA expression, such as miRNAs and siRNAs, could also influence DNA methylation or histone modifications (De Lucia & Dean, 2011; Zhao & Chen, 2014), further promoting chromatin accessibility at the *ACO1* locus. Histone marks, such as H3K4me3 (linked to active transcription) and H3K27me3 (associated with repression), may also be altered by genome doubling, facilitating an open chromatin state (Liu *et al.*, 2015; Han *et al.*, 2022). Increase in gene dosage following polyploidization can also influence epigenetic regulation by enhancing the recruitment of modifiers like histone enzymes and DNA methyltransferases. Together or independently, these modifications may stabilize the chromatin structure at *ACO1*, facilitating its sustained expression.

This study sheds new light on the role of polyploidization in enhancing plant resilience, revealing how genome doubling can lead to significant adaptations that improve a plant's ability to withstand environmental stresses. By understanding the molecular mechanisms behind this process, this research not only deepens our knowledge of evolutionary biology but also opens up exciting new avenues in plant breeding, offering the potential to develop crops with enhanced stress tolerance to changing environmental conditions. This could lead to more sustainable agricultural practices and a means to facing global challenges, such as climate change.

Acknowledgements

We thank Prof. Qi Xie from the Institute of Genetics and Development, Chinese Academy of Sciences, for providing the *YAO* promoter-driven CRISPR/Cas9 vector, our colleague Dr Robert M. Larkin from Huazhong Agricultural University, and Dr Olivier Martin from IPS2 (INRAE, France) for critical reading of the manuscript. This research was financially supported by grants from the National Key Research & Development Program of China (2024YFD1200501), the National Natural Science Foundation of China (32172525 and 32202432), the Foundation of Hubei Hongshan laboratory (2021hszd009), the China Agricultural Research System (CARS-26) and the Department of Science and Technology of Hubei Province (2022BBA0019). A. Bendahmane is funded by the ANR BioAdapt (ANR-21-LCV3-0003), LabEx Saclay Plant Sciences (SPS) (ANR-10-LABX-40-SPS), and the NectarGland ERC Project (101095736).

Competing interests

None declared.

Author contributions

W-WG, XS and F-QT designed the research. XS, MZ, T-TW, JR, Y-JF, Q-MX, H-XC, S-QZ and K-DX performed the experiments. Y-YD and MZ analyzed RNA-Seq data. MZ and HG analyzed whole-genome bisulfite sequencing data. MZ analyzed ATAC-Seq data. XS and F-QT wrote the manuscript. A Bendahmane, A Boualem, YH, FZ and X-MW improved the manuscript. XS and MZ contributed equally to this work.

ORCID

Abdelhafid Bendahmane https://orcid.org/0000-0003-3246-868X
Adnane Boualem https://orcid.org/0000-0003-4428-6496
Wen-Wu Guo https://orcid.org/0000-0002-2519-9672

Feng-Quan Tan https://orcid.org/0000-0003-3647-864X
Xiao-Meng Wu https://orcid.org/0000-0001-5798-5734

Data availability

All high-throughput sequencing data generated in this study have been deposited in the SRA database under the accession no.: PRJNA1159448, which includes the WGS-seq data, RNA-seq data, the BS-seq data and the ATAC-seq data. Source data are provided with this paper.

References

Achard P, Cheng H, De Grauwe L, Decat J, Schoutteten H, Moritz T, Van Der Straeten D, Peng J, Harberd NP. 2006. Integration of plant responses to environmentally activated phytohormonal signals. *Science* **311**: 91–94.

Allakhverdiev SI, Nishiyama Y, Miyairi S, Yamamoto H, Inagaki N, Kanesaki Y, Murata N. 2002. Salt stress inhibits the repair of photodamaged photosystem II by suppressing the transcription and translation of *psbA*genes in *Synechocystis*. *Plant Physiology* **130**: 1443–1453.

Allario T, Brumos J, Colmenero-Flores JM, Iglesias DJ, Pina JA, Navarro L, Talon M, Ollitrault P, Morillon R. 2013. Tetraploid Rangpur lime rootstock increases drought tolerance via enhanced constitutive root abscisic acid production. *Plant, Cell & Environment* **36**: 856–868.

Allario T, Brumos J, Colmenero-Flores JM, Tadeo F, Froelicher Y, Talon M, Navarro L, Ollitrault P, Morillon R. 2011. Large changes in anatomy and physiology between diploid Rangpur lime (*Citrus limonia*) and its autotetraploid are not associated with large changes in leaf gene expression. *Journal of Experimental Botany* **62**: 2507–2519.

Almeida DM, Oliveira MM, Saibo NJM. 2017. Regulation of Na^+ and K^+ homeostasis in plants: towards improved salt stress tolerance in crop plants. *Genetics and Molecular Biology* **40**: 326–345.

Booker MA, DeLong A. 2015. Producing the ethylene signal: regulation and diversification of ethylene biosynthetic enzymes. *Plant Physiology* **169**: 42–50.

Chao D-Y, Dilkes B, Luo H, Douglas A, Yakubova E, Lahner B, Salt DE. 2013. Polyploids exhibit higher potassium uptake and salinity tolerance in *Arabidopsis*. *Science* **341**: 658–659.

Chen ZJ. 2007. Genetic and epigenetic mechanisms for gene expression and phenotypic variation in plant polyploids. *Annual Review of Plant Biology* **58**: 377–406.

Dai W, Wang M, Gong X, Liu J-H. 2018. The transcription factor FcWRKY40 of *Fortunella crassifolia* functions positively in salt tolerance through modulation of ion homeostasis and proline biosynthesis by directly regulating *SOS2* and *P5CS1* homologs. *New Phytologist* **219**: 972–989.

Datta R, Kumar D, Sultana A, Hazra S, Bhattacharyya D, Chattopadhyay S. 2015. Glutathione regulates 1-aminocyclopropane-1-carboxylate synthase transcription via WRKY33 and 1-aminocyclopropane-1-carboxylate oxidase by modulating messenger RNA stability to induce ethylene synthesis during stress. *Plant Physiology* **169**: 2963–2981.

De Lucia F, Dean C. 2011. Long non-coding RNAs and chromatin regulation. *Current Opinion in Plant Biology* **14**: 168–173.

Del Pozo JC, Ramirez-Parra E. 2014. Deciphering the molecular bases for drought tolerance in Arabidopsis autotetraploids. *Plant, Cell & Environment* **37**: 2722–2737.

Delarue M, Benhamed M, Fragkostefanakis S. 2025. The role of epigenetics in tomato stress adaptation. *New Crops* **2**: 100044.

Ding M, Chen ZJ. 2018. Epigenetic perspectives on the evolution and domestication of polyploid plant and crops. *Current Opinion in Plant Biology* **42**: 37–48.

Dubois M, Van den Broeck L, Inzé D. 2018. The pivotal role of ethylene in plant growth. *Trends in Plant Science* **23**: 311–323.

Franks SJ. 2011. Plasticity and evolution in drought avoidance and escape in the annual plant *Brassica rapa*. *New Phytologist* **190**: 249–257.

Franks SJ, Sim S, Weis AE. 2007. Rapid evolution of flowering time by an annual plant in response to a climate fluctuation. *Proceedings of the National Academy of Sciences, USA* **104**: 1278–1282.

Galvan-Ampudia CS, Testerink C. 2011. Salt stress signals shape the plant root. *Current Opinion in Plant Biology* **14**: 296–302.

Galvan-Ampudia Carlos S, Julkowska Magdalena M, Darwish E, Gandullo J, Korver Ruud A, Brunoud G, Haring Michel A, Munnik T, Vernoux T, Testerink C. 2013. Halotropism is a response of plant roots to avoid a saline environment. *Current Biology* **23**: 2044–2050.

Gao H, Xiao GA, Bao Y, Xia QM, Xie KD, Wu XM, Guo WW. 2024. Integrative DNA methylome and transcriptome analysis illuminate leaf phenotype alterations in tetraploid citrus. *Horticulture Advances* **2**: 28.

Gayomba SR, Muday GK. 2020. Flavonols regulate root hair development by modulating accumulation of reactive oxygen species in the root epidermis. *Development* **147**: dev185819.

Gong Q, Li S, Zheng Y, Duan H, Xiao F, Zhuang Y, He J, Wu G, Zhao S, Zhou H *et al.* 2020. SUMOylation of MYB30 enhances salt tolerance by elevating alternative respiration via transcriptionally upregulating AOX1a in Arabidopsis. *The Plant Journal* **102**: 1157–1171.

Han J, Lopez-Arredondo D, Yu G, Wang Y, Wang B, Wall SB, Zhang X, Fang H, Barragán-Rosillo AC, Pan X *et al.* 2022. Genome-wide chromatin accessibility analysis unveils open chromatin convergent evolution during polyploidization in cotton. *Proceedings of the National Academy of Sciences, USA* **119**: e2209743119.

Hostetler AN, de Sousa M, Tinoco S, Sparks EE. 2023. Root responses to abiotic stress: a comparative look at root system architecture in maize and sorghum. *Journal of Experimental Botany* **75**: 553–562.

Hu C, Wei C, Ma Q, Dong H, Shi K, Zhou Y, Foyer CH, Yu J. 2021. Ethylene response factors 15 and 16 trigger jasmonate biosynthesis in tomato during herbivore resistance. *Plant Physiology* **185**: 1182–1197.

Huang X-S, Wang W, Zhang Q, Liu J-H. 2013. A basic helix-loop-helix transcription factor, *PtrbHLH*, of *Poncirus trifoliata* confers cold tolerance and modulates peroxidase-mediated scavenging of hydrogen peroxide. *Plant Physiology* **162**: 1178–1194.

Hummel I, Vile D, Violle C, Devaux J, Ricci B, Blanchard A, Garnier É, Roumet C. 2007. Relating root structure and anatomy to whole-plant functioning in 14 herbaceous Mediterranean species. *New Phytologist* **173**: 313–321.

Innan H, Kondrashov F. 2010. The evolution of gene duplications: classifying and distinguishing between models. *Nature Reviews Genetics* **11**: 97–108.

Irigoyen S, Ramasamy M, Pant S, Niraula P, Bedre R, Gurung M, Rossi D, Laughlin C, Gorman Z, Achor D *et al.* 2020. Plant hairy roots enable high throughput identification of antimicrobials against *Candidatus Liberibacter* spp. *Nature Communications* **11**: 5802.

Ivanchenko MG, Muday GK, Dubrovsky JG. 2008. Ethylene–auxin interactions regulate lateral root initiation and emergence in *Arabidopsis thaliana*. *The Plant Journal* **55**: 335–347.

Jourda C, Cardi C, Mbéguié-A-Mbéguié D, Bocs S, Garsmeur O, D'Hont A, Yahiaoui N. 2014. Expansion of banana (*Musa acuminata*) gene families involved in ethylene biosynthesis and signalling after lineage-specific whole-genome duplications. *New Phytologist* **202**: 986–1000.

Kim D, Paggi JM, Park C, Bennett C, Salzberg SL. 2019. Graph-based genome alignment and genotyping with HISAT2 and HISAT-genotype. *Nature Biotechnology* **37**: 907–915.

Klein SP, Schneider HM, Perkins AC, Brown KM, Lynch JP. 2020. Multiple integrated root phenotypes are associated with improved drought tolerance. *Plant Physiology* **183**: 1011–1025.

Köhler C, Dziasek K, Del Toro-De LG. 2021. Postzygotic reproductive isolation established in the endosperm: mechanisms, drivers and relevance. *Philosophical Transactions of the Royal Society of London. Series B: Biological Sciences* **376**: 20200118.

Kong D, Ma C, Zhang Q, Li L, Chen X, Zeng H, Guo D. 2014. Leading dimensions in absorptive root trait variation across 96 subtropical forest species. *New Phytologist* **203**: 863–872.

Lewis DR, Negi S, Sukumar P, Muday GK. 2011. Ethylene inhibits lateral root development, increases IAA transport and expression of PIN3 and PIN7 auxin efflux carriers. *Development* **138**: 3485–3495.

Li H, Durbin R. 2010. Fast and accurate long-read alignment with Burrows-Wheeler Transform. *Bioinformatics* **26**: 589–595.

Li H, Wang L, Liu M, Dong Z, Li Q, Fei S, Xiang H, Liu B, Jin W. 2020. Maize plant architecture is regulated by the ethylene biosynthetic gene *ZmACS7*. *Plant Physiology* **183**: 1184–1199.

Liang X, Li J, Yang Y, Jiang C, Guo Y. 2024. Designing salt stress-resilient crops: current progress and future challenges. *Journal of Integrative Plant Biology* **66**: 303–329.

Linkies A, Müller K, Morris K, Turečková V, Wenk M, Cadman CSC, Fo C, Strnad M, Lynn JR, Finch-Savage WE *et al.* 2009. Ethylene interacts with abscisic acid to regulate endosperm rupture during germination: a comparative approach using *Lepidium sativum* and *Arabidopsis thaliana*. *Plant Cell* **21**: 3803–3822.

Liu J, Osbourn A, Ma P. 2015. MYB transcription factors as regulators of phenylpropanoid metabolism in plants. *Molecular Plant* **8**: 689–708.

Liu X, Bie XM, Lin X, Li M, Wang H, Zhang X, Yang Y, Zhang C, Zhang XS, Xiao J. 2023. Uncovering the transcriptional regulatory network involved in boosting wheat regeneration and transformation. *Nature Plants* **9**: 908–925.

Lynch JP. 2022. Harnessing root architecture to address global challenges. *The Plant Journal* **109**: 415–431.

Ma Z, Guo D, Xu X, Lu M, Bardgett RD, Eissenstat DM, McCormack ML, Hedin LO. 2018. Evolutionary history resolves global organization of root functional traits. *Nature* **555**: 94–97.

Maxwell DP, Wang Y, McIntosh L. 1999. The alternative oxidase lowers mitochondrial reactive oxygen production in plant cells. *Proceedings of the National Academy of Sciences, USA* **96**: 8271–8276.

McKenna A, Hanna M, Banks E, Sivachenko A, Cibulskis K, Kernytsky A, Garimella K, Altshuler D, Gabriel S, Daly M *et al.* 2010. The Genome Analysis Toolkit: a MapReduce framework for analyzing next-generation DNA sequencing data. *Genome Research* **20**: 1297–1303.

Moya JL, Gómez-Cadenas A, Primo-Millo E, Talon M. 2003. Chloride absorption in salt-sensitive Carrizo citrange and salt-tolerant Cleopatra mandarin citrus rootstocks is linked to water use. *Journal of Experimental Botany* **54**: 825–833.

Negi S, Ivanchenko MG, Muday GK. 2008. Ethylene regulates lateral root formation and auxin transport in *Arabidopsis thaliana*. *The Plant Journal* **55**: 175–187.

Nguyen L-T, Schmidt HA, von Haeseler A, Minh BQ. 2015. IQ-TREE: a fast and effective stochastic algorithm for estimating maximum-likelihood phylogenies. *Molecular Biology and Evolution* **32**: 268–274.

Otto SP, Whitton J. 2000. Polyploid incidence and evolution. *Annual Review of Genetics* **34**: 401–437.

Panchy N, Lehti-Shiu M, Shiu S-H. 2016. Evolution of gene duplication in plants. *Plant Physiology* **171**: 2294–2316.

Qin Y-M, Hu C-Y, Pang Y, Kastaniotis AJ, Hiltunen JK, Zhu Y-X. 2007. Saturated very-long-chain fatty acids promote cotton fiber and arabidopsis cell elongation by activating ethylene biosynthesis. *Plant Cell* **19**: 3692–3704.

Roumet C, Urcelay C, Díaz S. 2006. Suites of root traits differ between annual and perennial species growing in the field. *New Phytologist* **170**: 357–368.

Sakamoto H, Maruyama K, Sakuma Y, Meshi T, Iwabuchi M, Shinozaki K, Yamaguchi-Shinozaki K. 2004. Arabidopsis cys2/his2-type zinc-finger proteins function as transcription repressors under drought, cold, and high-salinity stress conditions. *Plant Physiology* **136**: 2734–2746.

Schenk HJ, Jackson RB. 2002. Rooting depths, lateral root spreads and below-ground/above-ground allometries of plants in water-limited ecosystems. *Journal of Ecology* **90**: 480–494.

Schmidt R, Mieulet D, Hubberten H-M, Obata T, Hoefgen R, Fernie AR, Fisahn J, San Segundo B, Guiderdoni E, Schippers JHM *et al.* 2013. Salt-responsive ERF1 regulates reactive oxygen species–dependent signaling during the initial response to salt stress in rice. *Plant Cell* **25**: 2115–2131.

Shabala S, Cuin TA. 2008. Potassium transport and plant salt tolerance. *Physiologia Plantarum* **133**: 651–669.

Smalle J, Van Der Straeten D. 1997. Ethylene and vegetative development. *Plant Physiology* **100**: 593–605.

Smirnoff N, Arnaud D. 2019. Hydrogen peroxide metabolism and functions in plants. *New Phytologist* **221**: 1197–1214.

Soltis PS, Soltis DE. 2000. The role of genetic and genomic attributes in the success of polyploids. *Proceedings of the National Academy of Sciences, USA* **97**: 7051–7057.

Sun Y, Tian Z, Zuo D, Wang Q, Song G. 2024. GhUBC10-2 mediates GhGSTU17 degradation to regulate salt tolerance in cotton (*Gossypium hirsutum*). *Plant, Cell & Environment* **47**: 1606–1624.

Sweetman C, Waterman CD, Rainbird BM, Smith PMC, Jenkins CD, Day DA, Soole KL. 2019. AtNDB2 is the main external NADH dehydrogenase in mitochondria and is important for tolerance to environmental stress. *Plant Physiology* **181**: 774–788.

Tan F-Q, Tu H, Liang W-J, Long J-M, Wu X-M, Zhang H-Y, Guo W-W. 2015. Comparative metabolic and transcriptional analysis of a doubled diploid and its diploid citrus rootstock (*C. junos* cv. Ziyang xiangcheng) suggests its potential value for stress resistance improvement. *BMC Plant Biology* **15**: 89.

Tan F-Q, Tu H, Wang R, Wu X-M, Xie K-D, Chen J-J, Zhang H-Y, Xu J, Guo W-W. 2017. Metabolic adaptation following genome doubling in citrus doubled diploids revealed by non-targeted metabolomics. *Metabolomics* **13**: 143.

Tasdighian S, Van Bel M, Li Z, Van de Peer Y, Carretero-Paulet L, Maere S. 2017. Reciprocally retained genes in the angiosperm lineage show the hallmarks of dosage balance sensitivity. *Plant Cell* **29**: 2766–2785.

Trapnell C, Roberts A, Goff L, Pertea G, Kim D, Kelley DR, Pimentel H, Salzberg SL, Rinn JL, Pachter L. 2012. Differential gene and transcript expression analysis of RNA-seq experiments with TopHat and Cufflinks. *Nature Protocols* **7**: 562–578.

Van de Peer Y, Ashman T-L, Soltis PS, Soltis DE. 2020. Polyploidy: an evolutionary and ecological force in stressful times. *Plant Cell* **33**: 11–26.

Van de Peer Y, Mizrachi E, Marchal K. 2017. The evolutionary significance of polyploidy. *Nature Reviews Genetics* **18**: 411–424.

Van Zelm E, Zhang Y, Testerink C. 2020. Salt tolerance mechanisms of plants. *Annual Review of Plant Biology* **71**: 403–433.

Wang L, Cao S, Wang P, Lu K, Song Q, Zhao F-J, Chen ZJ. 2021. DNA hypomethylation in tetraploid rice potentiates stress-responsive gene expression for salt tolerance. *Proceedings of the National Academy of Sciences, USA* **118**: e2023981118.

Wang Z, Miao H, Liu J, Xu B, Yao X, Xu C, Zhao S, Fang X, Jia C, Wang J *et al.* 2019. *Musa balbisiana* genome reveals subgenome evolution and functional divergence. *Nature Plants* **5**: 810–821.

Yang SF, Hoffman NE. 1984. Ethylene biosynthesis and its regulation in higher plants. *Annual Review of Plant Biology* **35**: 155–189.

Yoshizumi T, Tsumoto Y, Takiguchi T, Nagata N, Yamamoto YY, Kawashima M, Ichikawa T, Nakazawa M, Yamamoto N, Matsui M. 2006. Increased level of polyploidy1, a conserved repressor of CYCLINA2 transcription, controls endoreduplication in *Arabidopsis*. *Plant Cell* **18**: 2452–2468.

Yu J, Zhu C, Xuan W, An H, Tian Y, Wang B, Chi W, Chen G, Ge Y, Li J *et al.* 2023. Genome-wide association studies identify OsWRKY53 as a key regulator of salt tolerance in rice. *Nature Communications* **14**: 3550.

Zhan A, Schneider H, Lynch JP. 2015. Reduced lateral root branching density improves drought tolerance in maize. *Plant Physiology* **168**: 1603–1615.

Zhang F, Rossignol P, Huang T, Wang Y, May A, Dupont C, Orbovic V, Irish VF. 2020. Reprogramming of stem cell activity to convert thorns into branches. *Current Biology* **30**: 2951–2961.

Zhang H, Zheng R, Wang Y, Zhang Y, Hong P, Fang Y, Li G, Fang Y. 2019. The effects of Arabidopsis genome duplication on the chromatin organization and transcriptional regulation. *Nucleic Acids Research* **47**: 7857–7869.

Zhang M, Tan F-Q, Fan Y-J, Wang T-T, Song X, Xie K-D, Wu X-M, Zhang F, Deng X-X, Grosser JW *et al.* 2022. Acetylome reprograming participates in the establishment of fruit metabolism during polyploidization in citrus. *Plant Physiology* **190**: 2519–2538.

Zhao Y, Chen X. 2014. Non-coding RNAs and DNA methylation in plants. *National Science Review* **1**: 219–229.

Zheng H, Dong L, Han X, Jin H, Yin C, Han Y, Li B, Qin H, Zhang J, Shen Q *et al.* 2020. The TuMYB46L-TuACO3 module regulates ethylene biosynthesis in einkorn wheat defense to powdery mildew. *New Phytologist* **225**: 2526–2541.

Zhou H, Zhao J, Yang Y, Chen C, Liu Y, Jin X, Chen L, Li X, Deng XW, Schumaker KS *et al.* 2012. Ubiquitin-specific protease16 modulates salt

tolerance in *Arabidopsis* by regulating Na^+/H^+ antiport activity and serine hydroxymethyltransferase stability. *Plant Cell* **24**: 5106–5122.

Zhu H, Chen C, Zeng J, Yun Z, Liu Y, Qu H, Jiang Y, Duan X, Xia R. 2020. MicroRNA528, a hub regulator modulating ROS homeostasis via targeting of a diverse set of genes encoding copper-containing proteins in monocots. *New Phytologist* **225**: 385–399.

Zhu Z, An F, Feng Y, Li P, Xue L, Mu A, Jiang Z, Kim JM, To TK, Li W *et al.* 2011. Derepression of ethylene-stabilized transcription factors (EIN3/EIL1) mediates jasmonate and ethylene signaling synergy in *Arabidopsis*. *Proceedings of the National Academy of Sciences, USA* **108**: 12539–12544.

Zou L, Liu W, Zhang Z, Edwards EJ, Gathunga EK, Fan P, Duan W, Li S, Liang Z. 2020. Gene body demethylation increases expression and is associated with self-pruning during grape genome duplication. *Horticulture Research* **7**: 84.

Supporting Information

Additional Supporting Information may be found online in the Supporting Information section at the end of the article.

Fig. S1 Morphological comparison of flowers, fruits, and seeds between tetraploids (4×) and their corresponding diploid (2×) progenitors.

Fig. S2 Leaf injury symptoms after treatment with different NaCl concentrations.

Fig. S3 Comparison of Na^+ content, K^+ content, and K^+ : Na^+ ratios between tetraploids (4×) and diploid (2×) plants.

Fig. S4 Tetraploid roots enhance salt stress resilience.

Fig. S5 qRT-PCR analysis of salt stress responsive maker genes in diploid (2×) and tetraploid (4×) roots from *Citrus* and *Poncirus* genera under NaCl treatment.

Fig. S6 Transcriptomic analysis of tetraploid (4×) and diploid (2×) roots from *Citrus* and *Poncirus* genera under NaCl treatment and control conditions.

Fig. S7 Motif enrichment in promoters of 847 upregulated genes in tetraploid (4×) roots relative to diploid (2×) roots across three genotypes.

Fig. S8 Phylogenetic tree and expression analysis of *ACO* genes in citrus.

Fig. S9 Ethylene treatment in diploid (2×) replicates the root phenotype and salt stress resilience in tetraploids.

Fig. S10 Validation of *ACO1* overexpression and knockout lines.

Fig. S11 RNA-seq and metabolic analysis of roots.

Fig. S12 Genome-wide DNA methylation profiling of tetraploid (4×) and diploid (2×) roots in *Citrus* and *Poncirus* genera.

Fig. S13 CHG and CHH DNA methylation across *ACO1* in roots of tetraploid (4×) and diploid (2×).

Fig. S14 Analysis of DNA methylation profiles across *ACO1* gene body in tetraploid (4×) and diploid (2×) using bisulfite sequencing PCR.

Fig. S15 ATAC-seq analysis of tetraploids (4×) and diploid (2×) roots under control conditions.

Fig. S16 Representative upregulated genes in tetraploid roots under salt treatment showing increased chromatin accessibility under control conditions.

Table S1 Summary of 11 accessions in Rutaceae family used in this study.

Table S2 Primers used in this study.

Table S3 Summary of next-generation sequencing data for *Citrus junos* (CJ), *Citrus reticulata* (CR), and *Poncirus trifoliata* (PT).

Table S4 Differentially expressed genes (DEGs) in *Citrus junos* tetraploid (CJ-4×) roots compared with diploid (CJ-2×) roots after salt treatment.

Table S5 Differentially expressed genes (DEGs) in *Citrus reticulata* tetraploid (CR-4×) roots compared with diploid (CR-2×) roots after salt treatment.

Table S6 Differentially expressed genes (DEGs) in *Poncirus trifoliata* tetraploid (PT-4×) roots compared with diploid (PT-2×) roots after salt treatment.

Table S7 Commonly regulated differentially expressed genes (DEGs) in tetraploid (4×) roots of *Citrus junos* (CJ-4×), *Citrus reticulata* (CR-4×), and *Poncirus trifoliata* (PT-4×) compared with their corresponding diploid (2×) roots after salt treatment.

Table S8 Differentially expressed genes (DEGs) in *Citrus junos* tetraploid (CJ-4×) roots compared with diploid (CJ-2×) roots under control conditions.

Table S9 Differentially expressed genes (DEGs) in *Citrus reticulata* tetraploid (CR-4×) roots compared with diploid (CR-2×) roots under control conditions.

Table S10 Differentially expressed genes (DEGs) in *Poncirus trifoliata* tetraploid (PT-4×) roots compared with diploid (PT-2×) roots under control conditions.

Table S11 Commonly regulated differentially expressed genes (DEGs) in tetraploid (4×) roots of *Citrus junos* (CJ-4×), *Citrus reticulata* (CR-4×), and *Poncirus trifoliata* (PT-4×) compared

with their corresponding diploid (2×) roots under control conditions.

Table S12 Differentially expressed genes (DEGs) in *ACO1*-overexpressing *Citrus junos* (*CjACO1*-OE) roots compared with wild-type (WT) roots under control conditions.

Table S13 Genes associated with differentially methylated regions (DMRs) between tetraploid (4×) and diploid (2×) roots of *Citrus reticulata* (CR).

Table S14 Genes associated with differentially methylated regions (DMRs) between tetraploid (4×) and diploid (2×) roots of *Citrus junos* (CJ).

Table S15 Genes associated with differentially methylated regions (DMRs) between tetraploid (4×) and diploid (2×) roots of *Poncirus trifoliata* (PT).

Table S16 Genes associated with differential accessible peaks in tetraploid (4×) roots compared with diploid (2×) roots of *Citrus reticulata* (CR).

Table S17 Genes associated with differential accessible peaks in tetraploid (4×) roots compared with diploid (2×) roots of *Poncirus trifoliata* (PT).

Please note: Wiley is not responsible for the content or functionality of any Supporting Information supplied by the authors. Any queries (other than missing material) should be directed to the *New Phytologist* Central Office.

Disclaimer: The New Phytologist Foundation remains neutral with regard to jurisdictional claims in maps and in any institutional affiliations.